

# A 3000 K laboratory emission spectrum of water

Pierre-François Coheur,

*Université Libre de Bruxelles, Service de Chimie Quantique et Photophysique,  
50 Av. F.D. Roosevelt, B-1050 Bruxelles, Belgium*

Peter F. Bernath,

*Department of Chemistry, University of Waterloo, Waterloo,  
ON Canada N2L 3G1 and Department of Chemistry,  
University of Arizona, Tucson, AZ, 85721*

Michel Carleer, Reginald Colin,

*Service de Chimie Quantique et Photophysique, Université Libre de Bruxelles,  
50 Av. F.D. Roosevelt, B-1050 Bruxelles, Belgium*

Oleg L. Polyansky,

*Sektion Spektren und Strukturdocumentation, University of Ulm,  
Helmholtzstraasse. 22, D-89069 Ulm, Germany*  
*Permanent address: Institute of Applied Physics, Russian Academy of Science,  
Uljanov Street 46, Nizhnii Novgorod, Russia 603950*

Nikolai F. Zobov, Sergei V. Shirin,

*Institute of Applied Physics, Russian Academy of Science,  
Uljanov Street 46, Nizhnii Novgorod, Russia 603950,  
and Department of Physics and Astronomy,  
University College London, London WC1E 6BT, UK*

Robert J. Barber and Jonathan Tennyson\*

*Department of Physics and Astronomy,  
University College London, London WC1E 6BT, UK*

(Dated: November 11, 2004)

## Abstract

A new emission spectrum of hot water with a temperature of about 3000 K is obtained using an oxy-acetylene torch. This spectrum contains a very large number of transitions. The spectrum, along with previous cooler laboratory emission spectra and an absorption spectrum recorded from a sunspot, is analysed in the 500 – 2000  $\text{cm}^{-1}$  region. Use of a newly calculated variational linelist for water allows significant progress to be made on assigning transitions involving highly-excited vibrational and rotational states. In particular, emission from rotationally-excited states up to  $J = 42$  and vibrational levels with up to 8 quanta of bending motion are assigned for the first time.

---

\*Electronic address: [j.tennyson@ucl.ac.uk](mailto:j.tennyson@ucl.ac.uk)

## I. INTRODUCTION

Vibration-rotation bands of hot water vapor are prominent in the spectra of flames and cool stars [1]. As early as the 1890's these "steam bands" were recorded from the infrared emission obtained during the combustion of hydrocarbons [2]. They can also be seen in rocket plumes and in jet engine exhausts [1]. Absorption of hot water vapor appears in the near infrared spectra of M-type stars [3] and brown dwarfs [4].

In the laboratory, the first modern data for hot water vapor were recorded by workers [5,6] at Meudon Observatory near Paris using an oxygen-hydrogen torch with a temperature of about 2900 K. The water emission in the 2800 – 9000  $\text{cm}^{-1}$  spectral region was recorded with a high resolution Fourier transform spectrometer. The rotational analysis was carried by the traditional methods of pattern recognition and combination differences. This pioneering effort provided some assignments up to  $J = 35$ , which lies at 11656  $\text{cm}^{-1}$  in the ground vibrational level.

The main difficulty in assigning the hot water spectrum, apart from dealing with an irregular jumble of lines from a light asymmetric top, is the presence of "anomalous centrifugal distortion". As the water molecule rotates, it experiences a substantial geometrical distortion, particularly of the bending angle, from centrifugal forces. The usual Watson rotational Hamiltonian diverges and an excessive number of centrifugal distortion terms need to be retained to fit the experimental data [7]. This divergence of the Hamiltonian limits the utility of predictions of line positions with higher  $J$  and, in particular, higher  $K_a$  values than those already included in the fit. It is this anomalous centrifugal distortion that limited the range of the rotational assignments in the original torch spectrum — not the signal-to-noise ratio of the spectra.

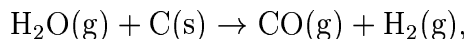
Various schemes [7-11] have been devised to reformulate the rotational Hamiltonian to improve convergence. These efforts have enjoyed some success, but the most satisfactory approach to assigning the hot water spectrum lies in abandoning perturbation theory altogether. The observation of the very dense water spectrum near 10  $\mu\text{m}$  in a sunspot [12] ("Water on the Sun") prompted the application of a variational approach [13] based on solving the full vibration-rotation Schroedinger equation to predict the energy levels with high quality *ab initio* potential surfaces [14, 15]. The variational approach has yielded the majority of the new assignments and energy levels as tabulated by Tennyson *et al.* [16].

Highly-excited levels of water can also be obtained through the analysis of overtone spectra. In contrast to the spectra obtained with furnaces and torches, the overtone data is rotationally cold. Overtone spectra have allowed the assignment of vibrational levels with up to 8 quanta of OH stretching (at  $25120\text{ cm}^{-1}$ ) to be observed [17]. Highly-excited bending levels, which are expected to show interesting effects [18,19], are not detected by overtone spectroscopy. The highest pure bending level that is reliably assigned [16] is (060), although tentative assignments of some levels up to (0 10 0) has been made on the basis of perturbations [20].

Very recently another source of highly-excited energy levels of water has been developed by Coudert *et al.* [21]. Coudert *et al.* have fitted the rotational energy levels obtained mainly from a far infrared emission spectrum of water vapor excited by a radio frequency discharge. The lines associated with the first eight vibrational levels were fitted with the theoretical approach of Coudert [11]. Very few new levels were seen, but the accuracy of the levels was significantly improved.

The goal of the current research is to obtain a new spectrum of a torch over a wider spectral range and then apply the variational approach to extend the assignments of the water levels to higher  $J, K_a$  levels. In addition, the torch spectrum allows us to assign new vibrational levels, particularly new pure bending levels.

The temperature of the water vapor in an oxy-acetylene or oxy-hydrogen torch can reach 3000 K, but the line width is about  $0.05 - 0.10\text{ cm}^{-1}$  because of pressure broadening at 1 atmosphere. The pressure can be reduced, but this also reduces the signal-to-noise ratio. The torch unfortunately has extensive emission from extraneous molecules such as CO, CO<sub>2</sub> and OH, in addition to water. Furnace sources allow the spectrum of pure water vapor to be recorded, but then the temperature is limited to a maximum of about 2000 K by the softening of the ceramic walls of the confining tube. Carbon tube furnaces can also reach 3000 K but the water gas reaction



prevents their use as a source of hot water emission. Despite its limitations, the oxy-acetylene torch at atmospheric pressure was used for all of the work reported in this paper. As shown below this approach yields a considerable amount of new information.

## II. EXPERIMENTAL PROCEDURE

Hot water vapour was produced in an oxy-acetylene torch at atmospheric pressure. Emission spectra of the flame were recorded using a Bruker IFS 120 M Fourier transform spectrometer between 500 and 13000  $\text{cm}^{-1}$ , using a variety of combinations of filters and detectors. For the 500 – 2000  $\text{cm}^{-1}$  region investigated here, two different settings were used: KBr entrance window and beamsplitter were used to record the spectra in the lower wavenumber region, along with a HgCdTe (MCT) detector. With this set-up, the entrance aperture was 4 mm in diameter and the spectral resolution was 0.03  $\text{cm}^{-1}$  (30 cm maximum optical path difference, mopd). A  $\text{CaF}_2$  window and beamsplitter were used to enhance the signal-to-noise ratio above 1900  $\text{cm}^{-1}$ , where an InSb detector was used. In that spectral region, a 2 mm aperture was chosen and the spectral resolution was set to 0.05  $\text{cm}^{-1}$  (18 cm mopd). In both regions 512 scans were co-added, thereby producing emission spectra with very low noise, see Fig. 1.

The line positions and intensities in the spectra have been determined using the WSPECTRA program [22]. In order to get rid of some weak ringing, the lines were first identified in spectra that were apodized using a Norton-Beer weak function. The fits were then performed on the unapodized spectra using the sinc instrument lineshape function to determine line positions and intensities, see Fig. 2. In the fitting procedure a Voigt molecular lineshape function was used, and both Gaussian and Lorentzian contributions were fitted. The WSPECTRA program also automatically fitted the baseline. It is worth pointing out that the spectra have not been corrected for the response of the optics and the detectors. The relative line intensities are therefore not reliable over large spectral ranges and should be used with care.

The wavenumber calibration was performed using the laboratory hot water vapor measurements of Tereszchuk *et al.* [23] in the 4880 – 7550  $\text{cm}^{-1}$  region, which is not presented in this paper. The consistency of the calibration was verified using the CO line positions in the 1-0 band, as archived by the National Institute of Standard and Technology [24]. Our measurements agree with the NIST data to within  $5 \times 10^{-3} \text{ cm}^{-1}$ , which is satisfactory considering the fact that the CO pressure-induced wavenumber shifts were not taken into account in the comparison. The value of  $5 \times 10^{-3} \text{ cm}^{-1}$  is taken as a “worst-case” estimate of the absolute accuracy of our measurements. A statistical uncertainty originating from

the quality of the spectral fit also has to be taken into account for each line. This statistical uncertainty is of the order of  $10^{-4} \text{ cm}^{-1}$  for strong and well-defined lines, but reaches significantly larger values for the numerous weak or blended lines.

As is obvious from Figs. 1 and 2, the spectra are very dense over the entire wavenumber region investigated, showing in addition to water lines, emission features of CO, CO<sub>2</sub> and OH. The OH lines were identified in the spectra by comparing the calibrated list of measured line positions between 5000 and 13000  $\text{cm}^{-1}$  to calculated values, obtained using the spectroscopic data of Colin *et al.* [25] and Melen *et al.* [26] Vibrational levels up to  $v = 8$  were considered in the comparison, and the very weak satellite lines were neglected. CO lines were similarly identified by using the HITEMP database [26] as a reference, with  $v = 8$  as the highest vibrational level, and both the <sup>12</sup>CO and <sup>13</sup>CO isotopes were considered. Observed CO lines are due to rotational transitions in the  $v = 0$  and 1 vibrational levels, with only 5 lines in the  $v = 2$  vibrational level.

A search for CO<sub>2</sub> lines was made using data taken from the CDS system of the Institute of Atmospheric Optics of the Siberian Branch of the Russian Academy of Sciences [28]. This database contains transitions from HITRAN, HITEMP and GEISA databases and can be used to simulate spectra at different temperatures, pressures, optical path lengths and lineshape parameters. It transpires that the CO<sub>2</sub> lines at 3000 K in the 500 – 2000  $\text{cm}^{-1}$  region are approximately 3 orders of magnitude weaker than the OH lines in this region. This means that contrary to our expectations, CO<sub>2</sub> lines are barely detectable in the spectrum analyzed in this paper. Indeed the only transitions identified lie below the cut-off used for measuring lines. The strong vibrational spectrum of CO<sub>2</sub> starts at about 2200  $\text{cm}^{-1}$  and will be taken into account in our future analysis of water molecule in the stretching mode region. In the region of interest in the current paper, out of the 10 100 measured lines, 363 were assigned to CO and 141 were assigned to pure rotational transitions of OH.

### III. THEORETICAL ANALYSIS

Spectra of hot water vapor in the 500 – 2000  $\text{cm}^{-1}$  region considered in this paper have been recorded in the laboratory (pure rotational spectrum  $T = 1800 \text{ K}$ , 373 – 934  $\text{cm}^{-1}$  region and  $\nu_2$  band spectrum  $T = 1800 \text{ K}$ , 933 – 2500  $\text{cm}^{-1}$  region) in emission and in sunspots ( $T \approx 3200 \text{ K}$ , 722 – 1011  $\text{cm}^{-1}$  region) in absorption [12,29,30]. It was decided

to analyze the current data along side these older spectra. Figure 3 compares a portion of these spectra.

The laboratory emission spectra from heated cells were recorded at a lower temperature than the present spectrum, so are less suitable for searching for highly-excited transitions of water. Indeed the previous  $\nu_2$  band spectrum contains some 40 % fewer lines than the oxy-acetylene torch spectrum. However in the  $373 - 934 \text{ cm}^{-1}$  region, the older emission spectrum has about 1000 more lines than the torch spectrum. The higher pressure in the torch spectrum means that many weak lines are obscured by stronger ones. The sunspot spectrum contains more than three times the number of lines, in absorption, than the present emission spectrum over the region in which they overlap. The sunspot spectrum thus remains the richest in terms of hidden information or number of lines per wavenumber. The main drawback of the sunspot spectrum is its limited wavenumber range due to absorptions in the Earth's atmosphere. Many of our newly assigned lines lie outside the range of the sunspot spectrum. Furthermore, the high density of the lines, up to 50 per wavenumber, requires very precise frequency predictions from theoretical calculations when dealing with the weaker lines. Almost all the strong and medium absorption lines were assigned in our previous work [13, 30], but few of the weaker lines.

These hot water spectra contain information on highly-excited vibrational and rotational levels. To be explicit, below we report emission arising from levels with up to 8 quanta of bending excitation and levels rotationally-excited to  $J = 42$ . Our theoretical model therefore must be capable of dealing with this high degree of excitation.

In analyzing the spectra we used a newly calculated variational linelist for hot water. The BT1 linelist was constructed explicitly to provide reliable models for the opacity of water in the atmospheres of cool stars. It therefore considered all levels of the molecule with  $J \leq 50$  and lying up to  $30\,000 \text{ cm}^{-1}$  above the  $J = 0$  ground state. The linelist used the recent, spectroscopically-determined potential energy surface of Shirin *et al.* [31] and special care was taken to ensure complete convergence of these levels as this has proved to be a problem with previous hot water linelists (see [30]). Full details of this linelist, including a database containing all 620 million transition intensities will be presented elsewhere [32].

The first step in analyzing the torch spectrum, after marking the OH and CO lines, was to make trivial assignments, that is assignments made using our new hot water linelist and previously known experimental energy levels of the water molecule [16]. As the observed line

widths are relatively large a significant number (about 20 %) of the experimental lines have double (or even triple) trivial assignments. In fact the number of multiply assigned lines was even higher after making our initial trivial assignments. In this initial analysis we used the theoretical linelist with an intensity cut-off about half that of the weakest experimental lines and did not compare theoretical and experimental intensities. In making our final trivial assignments we retained only lines which give at least 20 % of the total line intensity. About 80 % of the measured lines were assigned trivially.

In analyzing the remaining unassigned lines in the torch spectrum we employed different methods for different unknown levels. These levels can be roughly divided to three groups: (a) highest  $J$ , low  $K_a$  rotational levels in the lowest vibrational levels (000), (010) and (020), (b) high  $J$  ( $= 20 - 30$ ), intermediate and high  $K_a$ , low vibrational levels (000), (010), (020), (030) and (040) and (c) high bending levels (050), (060), (070) and (080).

For assigning transitions involving the highest  $J$  and low  $K_a$  rotational levels we used the method of branches, which has been described elsewhere [30,33]. To predict the energy of an unknown level we used not only the calculated value, but also looked at the difference between observed and calculated values for the same branch of levels with lower  $J$  values. The BT1 linelist is based on a spectroscopically-determined potential energy surface for which only levels with  $J = 0, 2$  and  $5$  were used in the fit. The standard deviation for that fit was  $0.1 \text{ cm}^{-1}$ , but for the highest  $J$  levels known previously the typical observed minus calculated (obs-calc) value grows to  $0.8 \text{ cm}^{-1}$  for (000) state,  $0.4 \text{ cm}^{-1}$  for (010) and  $0.3 \text{ cm}^{-1}$  for (020). Although these errors are much larger than the average spacing between measured lines, the differences increase smoothly with  $J$ . This means we can predict the positions of unknown higher  $J$  levels with an accuracy of about  $0.02 \text{ cm}^{-1}$ . This is sufficient for unambiguous assignments.

Some of the lines linking levels with the highest  $J$  values were found only in the laboratory pure rotational spectra [30], as they are obscured by stronger neighboring lines in the higher line width torch spectra. We were unable to assign these levels previously due to the lack of sufficiently accurate predictions from variational calculations. The present analysis allowed us to determine about 100 new levels and increase the maximum  $J$  value from 35 to 42 (from  $11656 \text{ cm}^{-1}$  to  $16406 \text{ cm}^{-1}$ ) for the ground vibrational level, from 32 to 39 for (010) and from 31 to 36 for (020). The newly determined highest  $J$ , low  $K_a$  rotational levels for the (000), (010) and (020) vibrational levels are presented in Table I.



TABLE I: Wavenumbers of the newly assigned highest  $J$  rotational levels in (000), (010) and (020) vibrational levels in  $\text{cm}^{-1}$ .

$J$	$K_a$	$K_c$	Level	$E$
36	0	36	000	12290.5959
36	1	36	000	12290.5959
36	1	35	000	12921.2711
36	2	35	000	12921.2711
36	2	34	000	13433.3356
36	3	34	000	13433.3356
36	3	33	000	13935.4309
36	4	33	000	13935.4309
36	20	17	000	19398.9036
36	20	16	000	19398.9036
36	21	16	000	19750.1982
36	21	15	000	19750.1982
36	22	15	000	20101.7967
36	22	14	000	20101.7967
36	23	14	000	20452.4935
36	23	13	000	20452.4935
37	0	37	000	12940.1441
37	1	37	000	12940.1441
37	1	36	000	13585.9949
37	2	36	000	13585.9949
37	2	35	000	14099.7715
37	3	35	000	14099.7715
37	3	34	000	14614.1750
37	4	34	000	14614.1750
37	24	14	000	21553.1329
37	24	13	000	21553.1329

38	0	38	000	13604.4879
38	1	38	000	13604.4879
38	1	37	000	14265.3170
38	2	37	000	14265.3170
38	2	36	000	14778.6740
38	3	36	000	14778.6740
38	3	35	000	15305.9609
38	4	35	000	15305.9609
39	0	39	000	14283.4348
39	1	39	000	14283.4348
39	1	38	000	14959.0419
39	2	38	000	14959.0419
39	2	37	000	15469.7102
39	3	37	000	15469.7102
39	3	36	000	16010.5323
39	4	36	000	16010.5323
40	0	40	000	14976.7975
40	1	40	000	14976.7975
40	1	39	000	15666.9690
40	2	39	000	15666.9690
40	2	38	000	16172.5357
40	3	38	000	16172.5357
41	0	41	000	15684.3814
41	1	41	000	15684.3814
41	1	40	000	16388.8934
41	2	40	000	16388.8934
42	0	42	000	16406.0561
42	1	42	000	16406.0561
33	0	33	010	11953.6676
33	1	33	010	11953.6676

33 1 32 010 12640.1170  
33 2 32 010 12640.1170  
33 2 31 010 13115.9905  
33 3 31 010 13115.9905  
33 3 30 010 13639.8400  
33 4 29 010 14085.0896  
33 7 26 010 15228.6773  
33 15 18 010 17420.0613  
33 16 17 010 17778.7798  
33 17 16 010 18130.4003  
33 18 15 010 18492.5424  
33 20 13 010 19211.6078  
33 21 13 010 19581.1881  
33 21 12 010 19581.1881  
33 22 12 010 19939.7786  
33 22 11 010 19939.7786  
33 24 10 010 20645.8124  
33 24 9 010 20645.8124  
34 0 34 010 12557.4625  
34 1 34 010 12557.4625  
34 1 33 010 13264.2962  
34 2 33 010 13264.2962  
35 0 35 010 13177.6869  
35 1 35 010 13177.6869  
35 1 34 010 13904.3971  
35 2 34 010 13904.3971  
36 0 36 010 13814.3780  
36 1 36 010 13814.3780  
36 1 35 010 14560.2728  
36 2 35 010 14560.2728

37	0	37	010	14467.5545
37	1	37	010	14467.5545
37	1	36	010	15231.8067
37	2	36	010	15231.8067
37	2	35	010	15653.8554
37	3	35	010	15653.8554
38	0	38	010	15137.1779
38	1	38	010	15137.1779
39	0	39	010	15823.2561
39	1	39	010	15823.2561
32	0	32	020	12913.3436
32	1	32	020	12913.3436
33	0	33	020	13511.4038
33	1	33	020	13511.4038
34	0	34	020	14128.3021
34	1	34	020	14128.3021
35	0	35	020	14763.9356
35	1	35	020	14763.9356
36	0	36	020	15418.0188
36	1	36	020	15418.0188

---

The majority of newly assigned levels belong to states with high  $J$  ( $= 20 - 30$ ), intermediate or high  $K_a$ , and low bending vibrational excitation. Within a set of levels with a given  $J$  and vibrational state the obs–calc changes smoothly with changing values of  $K_a$  and  $K_c$ . This means one can predict unknown levels with an accuracy sufficient for assignments. Our previous work on hot water spectra gave us enough known levels for each set to make this method of assignment possible. Our newly determined energy levels are given in the EPAPS archive [34].

Most newly determined levels in the two groups mentioned above were obtained from a single pure rotational transition, as in each case this line is the strongest for the level. It should be noted that the corresponding vibration-rotation transitions are largely not present

in the torch spectrum as such transitions involving levels with high  $K_a$  are too weak to be seen.

The fitting procedure employed to obtain the spectroscopically-determined potential [31] used experimental energy levels for bending states up to (060). For levels belonging to the (040), (050) and (060) vibrational levels the residuals of the fit were small and changed smoothly with quantum numbers. Assignments could therefore be made using theoretical predictions. Most newly determined levels were confirmed by combination differences, making them reliable. About 20 levels of the (070) bending level have been previously determined from overtone spectroscopy [20,35], along with the  $6_{34}$  level of the (080) vibrational level [20]. As these levels were not used in fitting, the residuals for them grows to  $0.5 \text{ cm}^{-1}$  for (070) and  $1 \text{ cm}^{-1}$  for (080). This is due to the bending vibrational levels approaching the barrier to linearity. Furthermore, for these states the obs–calc depends significantly on the value of  $K_a$  but has almost no dependence on  $J$  for a given  $K_a$ . This allowed us to assign 17 additional levels in (070) and 9 in (080). The assignments to (070) can be considered as reliable, especially those confirmed by combination differences. The assignments involving (080) are more tentative. The newly assigned rotational levels in the (060), (070) and (080) vibrational levels are presented in Table II.

TABLE II: Wavenumbers for rotational term values in the (060), (070) and (080) vibrational levels in  $\text{cm}^{-1}$ .

$J$	$K_a$	$K_c$	Level	$E$
0	0	0	060	8869.9538
1	1	1	060	8998.0996
1	1	0	060	9004.6170
2	2	1	060	9271.2847
3	1	2	060	9139.0734
3	2	1	060	9344.3799
3	3	0	060	9628.7737
4	2	3	060	9438.2526 <sup>a</sup>
4	3	2	060	9725.7365
4	4	1	060	10049.2800

5	0	5	060	9210.1607
5	1	4	060	9377.2237
5	2	4	060	9556.7927 <sup>a</sup>
5	2	3	060	9565.5203
5	3	2	060	9847.2247
5	4	2	060	10171.0870
5	4	1	060	10171.2898
5	5	1	060	10519.2778 <sup>b</sup>
5	5	0	060	10519.2778 <sup>b</sup>
6	1	6	060	9400.6406
6	1	5	060	9533.5828
6	2	5	060	9698.0404 <sup>b</sup>
6	2	4	060	9714.4540
6	3	4	060	9991.0166
6	3	3	060	9992.3307
6	4	3	060	10316.3808
6	5	2	060	10666.2485
7	0	7	060	9487.9479
7	1	6	060	9714.7602
7	3	4	060	10162.1936
7	4	4	060	10484.2790
7	4	3	060	10486.3693 <sup>a</sup>
7	5	2	060	10837.7072
7	6	2	060	11199.7595
7	6	1	060	11199.7370
7	7	1	060	11564.2145
7	7	0	060	11564.2145
8	1	8	060	9697.2256
8	2	7	060	10047.3069 <sup>a</sup>
8	3	6	060	10348.1658

8 3 5 060 10356.0418<sup>b</sup>  
8 4 5 060 10672.4910  
8 4 4 060 10678.8623<sup>b</sup>  
8 5 4 060 11032.0251  
8 5 3 060 11032.4511<sup>a</sup>  
8 6 3 060 11395.4898  
8 6 2 060 11394.9593  
8 8 1 060 12263.3487  
9 1 8 060 10143.6997  
9 2 8 060 10254.3984  
9 3 7 060 10558.6984<sup>b</sup>  
9 3 6 060 10574.3192  
9 4 5 060 10894.2476<sup>b</sup>  
9 6 4 060 11612.7597  
9 6 3 060 11613.0694<sup>b</sup>  
10 1 10 060 10069.0056<sup>a</sup>  
10 2 9 060 10483.2868  
10 3 8 060 10785.3000  
10 4 7 060 11143.4201<sup>a</sup>  
10 6 5 060 11853.8368  
10 8 3 060 12720.4711  
10 8 2 060 12720.4944  
11 0 11 060 10259.4551  
11 1 11 060 10283.9173<sup>a</sup>  
11 1 10 060 10656.5089  
11 2 9 060 10826.3404<sup>b</sup>  
11 3 8 060 11084.3958<sup>b</sup>  
11 4 7 060 11392.2185<sup>b</sup>  
11 5 6 060 11755.8094<sup>b</sup>  
12 1 12 060 10518.0698

12 1 11 060 10942.1613<sup>b</sup>  
12 2 11 060 11003.6709<sup>a</sup>  
12 2 10 060 11112.0853<sup>b</sup>  
12 3 10 060 11326.8032<sup>a</sup>  
12 4 9 060 11676.3099<sup>b</sup>  
12 5 8 060 12038.3255<sup>b</sup>  
13 0 13 060 10756.2885  
13 1 13 060 10773.1396<sup>b</sup>  
13 1 12 060 11246.8263<sup>a</sup>  
13 2 11 060 11411.2944<sup>b</sup>  
13 3 10 060 11690.6398<sup>a</sup>  
13 5 8 060 12356.5256  
14 0 14 060 11036.1947<sup>b</sup>  
14 1 14 060 11043.9614  
14 2 13 060 11607.5558<sup>a</sup>  
15 0 15 060 11330.4470<sup>b</sup>  
16 0 16 060 11654.8647<sup>b</sup>  
16 1 16 060 11658.8880<sup>a</sup>  
17 0 17 060 12004.1736<sup>b</sup>  
1 1 1 070 10334.3666  
1 1 0 070 10341.0547  
2 1 2 070 10374.8919  
2 2 1 070 10703.3386<sup>a</sup>  
3 0 3 070 10224.5606<sup>b</sup>  
3 1 3 070 10435.5297  
3 1 2 070 10475.6581  
3 2 1 070 10775.3009  
3 3 0 070 11136.7986<sup>b</sup>  
4 1 4 070 10516.1570  
4 1 3 070 10582.9251



4 2 3 070 10871.3547<sup>a</sup>  
4 3 2 070 11233.8187<sup>b</sup>  
5 1 5 070 10616.7746  
5 1 4 070 10716.5816<sup>a</sup>  
5 2 4 070 10990.9667  
5 2 3 070 10990.1665<sup>b</sup>  
6 1 6 070 10737.4070  
6 1 5 070 10875.8198  
6 2 5 070 11134.1762  
6 3 4 070 11496.9058<sup>b</sup>  
7 1 7 070 10878.1735  
7 1 6 070 11060.8235  
7 2 6 070 11300.7657<sup>b</sup>  
7 3 5 070 11660.8681  
7 3 4 070 11666.9403  
8 0 8 070 10897.3083<sup>b</sup>  
8 1 8 070 11039.2005  
8 1 7 070 11270.5126<sup>a</sup>  
8 2 7 070 11490.4559<sup>a</sup>  
8 2 6 070 11482.0729  
9 1 9 070 11221.7144  
9 1 8 070 11504.7708<sup>b</sup>  
9 2 7 070 11689.3420  
10 1 10 070 11424.9390<sup>a</sup>  
10 2 9 070 11938.9806<sup>a</sup>  
10 3 8 070 12302.1714<sup>b</sup>  
11 0 11 070 11573.2541<sup>b</sup>  
11 1 10 070 12043.1979<sup>a</sup>  
11 4 7 070 13778.6454  
12 0 12 070 11779.5362

12	2	11	070	12479.7768 <sup>b</sup>
13	0	13	070	12064.1500
2	2	1	080	12148.2928 <sup>b</sup>
3	0	3	080	11390.5763 <sup>b</sup>
3	1	2	080	11813.6815 <sup>b</sup>
4	1	4	080	11851.5431 <sup>b</sup>
6	2	5	080	12585.1205 <sup>b</sup>
7	1	6	080	12417.0858 <sup>a</sup>
9	1	8	080	12880.4466 <sup>a</sup>
10	1	10	080	12769.9046 <sup>a</sup>
10	2	9	080	13416.0819 <sup>b</sup>
11	1	10	080	13443.8321 <sup>b</sup>

---

<sup>a</sup> New levels confirmed by combination differences.

<sup>b</sup> New levels obtained from one transition.

For the (070) and (080) bending levels no transitions have been observed to the  $0_{00}$  rotational level. However it is possible to obtain an estimate for the vibrational band origin for these two levels by looking at the systematic differences between the observed and calculated rotational term values. Table III presents estimates for these band origins and a summary of the energy levels newly determined in this work. A complete tabulation of these levels is given in the EPAPS archive [34].

The many trivial assignments made in this work can be used to gauge the accuracy with which any new energy levels are determined. For strong lines the trivial assignments agree with the line position with a typical error of  $0.003 \text{ cm}^{-1}$ . This error is thus appropriate for the high  $J$ , intermediate or high  $K_a$ , and low bending vibrational excitation levels assigned here. For weaker transitions this level of agreement drops and the new high  $J$  levels and high bending levels are probably only accurate to about  $0.01 \text{ cm}^{-1}$ .

The EPAPS archive also contains a listing of the three spectra of hot water (re-)analyzed here: the new oxy-acetylene torch spectrum obtained with  $T = 3000 \text{ K}$  for the  $529 - 2000 \text{ cm}^{-1}$  region, the pure rotational laboratory emission spectrum  $T = 1800 \text{ K}$ ,  $373 - 934 \text{ cm}^{-1}$  region, and the sunspot absorption spectrum  $T \approx 3200 \text{ K}$ ,  $722 - 1011 \text{ cm}^{-1}$

region [12,29,30]. After completing work on the torch spectrum we performed a trivial assignment of the sunspot spectrum and then checked for consistency between theoretical and experimental intensities. Incorrect trivial assignments, those for which the theoretical line was too weak for a relatively strong experimental line, were removed. Even with OH and SiO lines marked, about half of measured lines in the sunspot spectrum remain unassigned. Assignments obtained from the torch spectrum have also been added to the pure rotational laboratory spectrum.

TABLE III: Summary of new rotational energy levels for each vibrational level. Experimental origins [16], number of new levels,  $N$ , and maximum  $J$  value.

Level	$E$	$N$	$J$
000	0.000	179	42
010	1594.746	149	39
020	3151.630	75	36
030	4666.790	14	22
040	6134.015	24	21
050	7542.437	58	20
060	8869.954	37	17
070	10085.9(2)	17	12
080	11253.8(5)	9	11

#### IV. CONCLUSIONS

In this paper we report the observation of a new spectrum obtained from an oxy-acetylene torch with a temperature of about 3000 K. This spectrum is rich in emission from hot water and, in principle, contains a significant quantity of new information.

A new, more accurate and more extensive, variational linelist has been used to analyze the torch spectrum with different strategies employed for transitions involving three different types of highly-excited states. Altogether about 85 % of the 10 100 lines measured in the torch spectrum in the 500 – 2000  $\text{cm}^{-1}$  range have been assigned. The majority of the

remaining unassigned lines lie in pure rotational transition region ( $500 - 1000 \text{ cm}^{-1}$ ). These lines belong mostly to high  $J$  rotational transitions within vibrational states with stretching excitation. Some of these lines could, in principal, be assigned now. However a more productive strategy is to analyze these transitions at the same time as the  $2000 - 5000 \text{ cm}^{-1}$  region, which contains the stretching vibration-rotation transitions. This approach will give combination differences to confirm the assignments made.

The bending region ( $1000 - 2000 \text{ cm}^{-1}$ ) contains further information on the higher bending states. To make progress on these highly-excited bending states will require an improved fit to the potential energy surface to give more reliable predictions. One method is to include iteratively the newly-determined energy levels of the high-lying bending states to give better predictions and hence more levels. This method has recently been used to analyze successfully the emission spectrum of hot (1800 K)  $\text{D}_2\text{O}$  [36].

## ACKNOWLEDGEMENTS

Financial support provided by the Fonds National de la Recherche Scientifique (F.N.R.S., Belgium, F.R.F.C. convention No 2.4536.01) and the "Actions de Recherches Concertees" (Communaute Francaise de Belgique) is acknowledged. This work was also supported by The Royal Society, INTAS, the UK Engineering and Physical Science Research Council, the NASA astrophysics program, the Canadian Natural Sciences and Engineering Council and the Russian Fund for Fundamental Studies.

## REFERENCES

1. P. F. Bernath, *Phys. Chem. Chem. Phys.* 4, 1501 (2002).
2. A. G. Gaydon, *The Spectroscopy of Flames*, 2nd edition, Chapman and Hall, London, 1974.
3. S.K. Leggett, F. Allard, C. Dahn, P.H. Hauschildt, T.H. Kerr and J. Rayner, *Astrophys. J.*, 535, 965 (2000).
4. J.D. Kirkpatrick, I.N. Reid, J. Liebert, R.M. Cutri, B. Nelson, C.A. Beichman, C.C. Dahn, D.G. Monet, J.E. Gizis and M.F. Skrutskie, *Astrophys. J.*, 519, 802 (1999).

5. J.-M. Flaud, C. Camy-Peyret and J.-P. Maillard, *Mol. Phys.*, **32**, 499 (1976).
6. C. Camy-Peyret, J.-M. Flaud, J.-P. Maillard and G. Guelachvili, *Mol. Phys.*, **33**, 1641 (1977).
7. O. L. Polyansky, *J. Mol. Spectrosc.* **112**, 79 (1985).
8. V.I. Starikov and S.N. Mikhailenko, *J. Phys. B*, **33**, 2141 (2000).
9. P. Chen, J.C. Pearson, H.M. Pickett, S. Matsuura and G.A. Blake, *Astrophys. J. Suppl.*, **128**, 371 (2000).
10. V.I.G. Tyuterev, *J. Mol. Spectrosc.*, **151**, 97 (1992).
11. R. Lanquetin, L. H. Coudert and C. Camy-Peyret, *J. Mol. Spectrosc.* **206**, 83 (2001).
12. L. Wallace, P. Bernath, W. Livingston, K. Hinkle, J. Busler, B. Guo and K.-Q. Zhang, *Science*, **268**, 1155 (1995).
13. O.L. Polyansky, N.F. Zobov, S. Viti, J. Tennyson, P.F. Bernath and L. Wallace, *Science*, **277**, 346 (1997).
14. H. Partridge and D.W. Schwenke, *J. Chem. Phys.*, **106**, 4618 (1997).
15. O. L. Polyansky, A. G. Csaszar, S. V. Shirin, N. V. Zobov, P. Bartletta, J. Tennyson, D. W. Schwenke and P. J. Knowles, *Science*, **299**, 539 (2003).
16. J. Tennyson, N.F. Zobov, R. Williamson, O.L. Polyansky and P.F. Bernath, *J. Phys. Chem. Ref. Data*, **30**, 735 (2001).
17. N.F. Zobov, D. Belmiloud, O.L. Polyansky, J. Tennyson, S.V. Shirin, M. Carleer, A. Jenouvrier, A.-C. Vandaele, P. F. Bernath, M.F. Mérienne and R. Colin, *J. Chem. Phys.*, **113**, 1546 (2000).
18. J.P. Rose and M.E. Kellman, *J. Chem. Phys.*, **105**, 7348 (1996).
19. M.S. Child, T. Weston and J. Tennyson, *Mol. Phys.*, **96**, 371 (1999).
20. A. Bykov, O. Naumenko, L. Sinitsa, B. Voronin, J.-M. Flaud, C. Camy-Peyret and R. Lanquetin, *J. Mol. Spectrosc.*, **205**, 1 (2001).

21. L. H. Coudert, O. Pirali, M. Vervloet, R. Lanquetin and C. Camy-Peyret, *J. Mol. Spectrosc.* (in press).
22. M. Carleer, *Wspectra: A Windows program to measure accurately the line intensities of high resolution Fourier Transform spectra.* in *Remote Sensing of Clouds and the Atmosphere.* ed. J.E. Russel, K. Schfer, and O. Lado-Bordowski, Vol. V. p. 337-342 2001: EOS/SPIE Proceedings series.
23. K. Tereszchuk, P.F. Bernath, N.F. Zobov, S.V. Shirin, O.L. Polyansky, N.I. Libeskind, J. Tennyson, and L. Wallace, *Astrophys. J.*, 577, 496 (2002).
24. A. G. Maki and J. S. Wells, <http://physics.nist.gov/PhysRefData/wavenum/html/contents.html>.
25. R. Colin, P.-F. Coheur, M. Kiseleva, A.C. Vandaele, and P.F. Bernath, *J. Mol. Spectrosc.*, 214, 225 (2002).
26. F. Melen, A. J. Sauval, N. Grevesse, C. B. Farmer, Ch. Servais, L. Delbouille, and G. Roland, *J. Mol. Spectrosc.*, 174, 490 (1995).
27. L.S. Rothman, C. Camy-Peyret, J.-M. Flaud, R.R. Gamache, A. Goldman, D. Goorvitch, R.L. Hawkins, J. Schroeder, J.E.A. Selby, and R.B. Wattson, HITEMP, the high-temperature molecular spectroscopic database. Private communication.
28. see <http://spectra.iao.ru>.
29. N.F. Zobov, O.L. Polyansky, J. Tennyson, J.A. Lotoski, P. Colarusso, K.-Q. Zhang and P.F. Bernath, *J. Mol. Spectrosc.*, 193, 118 (1999).
30. O.L. Polyansky, N.F. Zobov, S. Viti, J. Tennyson, P.F. Bernath and L. Wallace, *J. Mol. Spectrosc.*, 186, 422 (1997).
31. S.V. Shirin, O.L. Polyansky, N.F. Zobov, P. Barletta and J. Tennyson, *J. Chem. Phys.*, 118, 2124 (2003).
32. R.J. Barber and J. Tennyson, to be published.
33. O.L. Polyansky, N.F. Zobov, S. Viti, J. Tennyson, P.F. Bernath and L. Wallace, *Astrophys. J.*, 489, L205 (1997).

34. AIP electronic archive E-PAPS. Electronic versions of all the torch spectrum between 500 and 2000  $\text{cm}^{-1}$ , plus assignments, as well the 373 – 933  $\text{cm}^{-1}$  laboratory spectrum and the 722 – 1011  $\text{cm}^{-1}$  sunspot spectrum with updated assignments. Newly determined energy levels for vibrational states ( $0\nu_20$ ) with  $\nu_2 = 0 - 8$  are also given. These files can be retrieved from [ftp://ftp.aip.org/epaps/journ\\\_chem\\\_phys/](ftp://ftp.aip.org/epaps/journ\_chem\_phys/) using file name JCPA-1??-????-?.
35. O. Naumenko and A. Campargue, *J. Mol. Spectrosc.*, 221, 221 (2003).
36. S.V. Shirin, N.F. Zobov, O.L. Polyansky, J. Tennyson, T. Parekunnel and P.F. Bernath, *J. Chem. Phys.*, 120, 206 (2004).

## Figure Captions

FIG. 1 Raw emission spectrum of the oxy-acetylene flame in the  $500 - 2500 \text{ cm}^{-1}$  spectral region.

FIG.2 Example of a WSPECTRA fit of our data. The black line and grey line are, respectively, the observed and the calculated spectrum, with the residuals below on an expanded scale.

FIG. 3 Lower panel: Sunspot absorption (upper trace) and laboratory emission from heated cell spectra (lower trace) from work [30] near  $840 \text{ cm}^{-1}$ . Upper panel: Torch spectrum in the same region; vertical lines denote assigned transitions.